



DACA-GRPO: Denoising-Aware Credit Assignment for Reinforcement Learning in Diffusion Language Models

Amin Karimi Monsefi^{1,2,†,‡}, Dominic Culver^{2,†}, Nikhil Bhendawade², Lokesh Boominathan², Manuel R. Ciosici², Yizhe Zhang², Irina Belousova²

¹The Ohio State University ²Apple

Diffusion large language models are a compelling alternative to autoregressive models, yet existing RL methods for diffusion treat all denoising steps as equally important and rely on biased, high-variance likelihood estimates. We identify two fundamental weaknesses: the absence of *temporal credit assignment* across the denoising trajectory, and the systematic bias of mean-field likelihood estimates used for policy optimization. To address these, we propose Denoising-Aware Credit Assignment for GRPO (DACA-GRPO), a lightweight, plug-and-play enhancement for any GRPO-style trainer. DACA-GRPO introduces two complementary mechanisms: *Denoising Progress Scores*, which extract per-token importance weights from intermediate predictions at no additional forward cost, and *Stratified Masking Likelihood*, which partitions token positions into strata so that each token is predicted with most of the sequence as context, reducing the mean-field bias. Applied on top of three GRPO base methods, DACA-GRPO achieves consistent improvements across seven benchmarks spanning mathematical reasoning, code generation, constraint satisfaction, and constrained generation, with gains of up to 5.6pp on math reasoning, 7.4pp on code generation, 36.3pp on constraint satisfaction, and 5.9pp on JSON schema adherence.

Correspondence: Amin Karimi Monsefi: karimimonsefi.1@osu.edu; Dominic Culver: dominic_culver@apple.com; Irina Belousova: ibelousova@apple.com

Date: May 19, 2026

1 Introduction

Diffusion large language models (dLLMs) are an alternative paradigm to autoregressive models, supporting high-throughput, any-order parallel text generation. They operate by iteratively denoising corrupted sequences, starting from a sequence of mask or uniform tokens (Sahoo et al., 2024; Nie et al., 2026; Monsefi et al., 2026; Labs et al., 2025; Ye et al., 2025).

Group Relative Policy Optimization (Guo et al., 2025; Yu et al., 2025; Liu et al., 2025) (GRPO), now a standard post-training method for autoregressive LLMs, has recently been adapted to discrete diffusion models (Zhao et al., 2025; Tang et al., 2026; Rojas et al., 2026; Gong et al., 2025). Unlike autoregressive LLMs, dLLMs cannot directly compute the completion log-likelihood $\log p_\theta(o|q)$, so it must be approximated or replaced with an evidence lower bound (ELBO).

While these methods have seen significant success, they ignore the *denoising trajectory* itself. During generation, dLLMs compute distributions over every masked position at each step but unmask only a few; the remaining predictions—encoding the model’s evolving understanding—are discarded. Not all steps contribute equally: some involve decisive structural commitments, while others are routine fill-in. Yet current methods

[†]Equal contribution.

[‡]The Ohio State University. Work done during the internship at Apple.

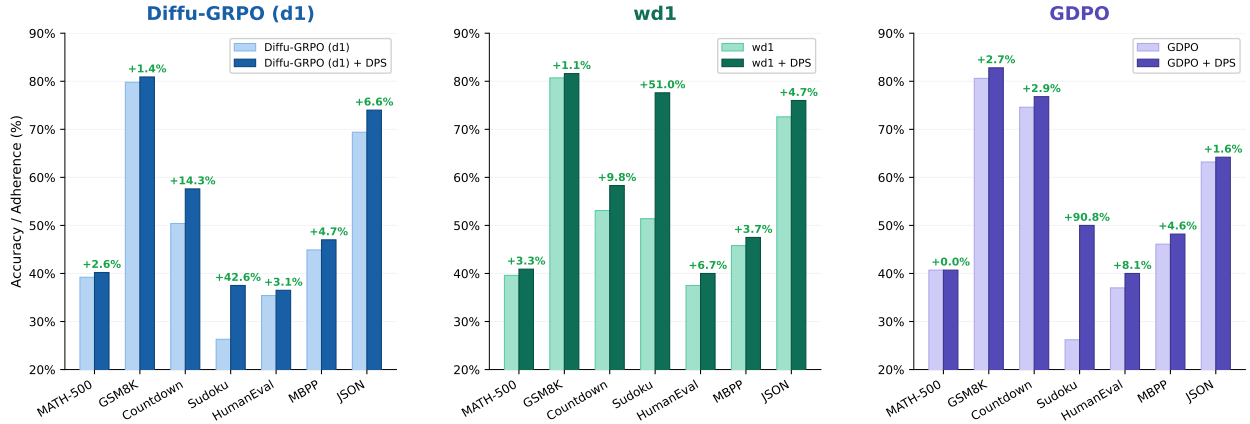


Figure 1 DPS improves all three base methods across all benchmarks. Best accuracy (%) across generation lengths $\{128, 256, 512\}$. Light bars: reproduced baselines. Dark bars: with DPS applied. Green percentages show relative improvement over the baseline. DPS delivers consistent gains across mathematical reasoning, code generation, constraint satisfaction, and constrained generation tasks, with the largest relative gains on Sudoku—up to +51% for wd1 and +90% for GDPO.

assign equal credit to every token regardless of when or how confidently it was generated. Moreover, the likelihood estimates suffer from mean-field bias—predicting all tokens from zero inter-token context—corrupting the policy gradient. We make the following contributions:

1. We **identify two fundamental weaknesses** in existing dLLM RL methods: the absence of temporal credit assignment across denoising steps, and the systematic bias of mean-field likelihood estimates used for policy optimization.
2. **Denoising Progress Scores (DPS)** track the model’s belief evolution across denoising steps, converting these signals into per-token importance weights that modulate the RL loss. DPS requires *no additional forward passes*—it repurposes logits that the model would otherwise discard.
3. To mitigate the likelihood bias, we introduce **Stratified Masking Likelihood (SML)**, a position-stratified estimator that partitions output tokens into K strata and evaluates each token with $(K-1)/K$ of the sequence as context. Intuitively, this should reduce the noise introduced by using the mean-field approximation by ensuring that token interdependency is captured amongst the strata.
4. **DACA-GRPO** combines DPS and SML into a unified, plug-and-play framework that is agnostic to the underlying GRPO variant.

We evaluate DACA-GRPO on top of three popular RL methods—Diffu-GRPO (Zhao et al., 2025), wd1 (Tang et al., 2026), and GDPO (Rojas et al., 2026)—across seven benchmarks spanning mathematical reasoning (MATH-500, GSM8K), code generation (MBPP, HumanEval), constraint satisfaction (Countdown, Sudoku), and constrained generation (JSON). DACA-GRPO delivers consistent improvements across benchmarks and base methods, with gains of up to 5.6pp on math reasoning, 7.4pp on code generation, 36.3pp on constraint satisfaction, and 5.9pp on JSON schema adherence. The two components are complementary: DPS is most impactful on structured constraint tasks and short generation lengths, while SML provides the largest gains on long-form math and code tasks.

2 Related work

Diffusion language models like MDLM (Sahoo et al., 2024) and LLaDA (Nie et al., 2026) established masked diffusion as a viable text generation paradigm, and subsequent work has applied direct preference optimization to this setting (Black et al., 2024; Xie et al., 2025; Lou et al., 2024). Our work is orthogonal to the diffusion architecture; we focus on the RL training signal.

Reinforcement learning has been widely applied to autoregressive LLMs through methods like Reinforcement Learning from Human Feedback (Ouyang et al. (2022)) and GRPO (Shao et al., 2024). Recent work extends GRPO to diffusion models: Diffu-GRPO (Zhao et al., 2025) adapts PPO-clipped objectives, wd1 (Tang et al., 2026) proposes a ratio-free alternative, GDPO (Rojas et al., 2026) formulates diffusion-specific policy optimization, and DiffuCoder (Gong et al., 2025) introduces coupled sampling for variance reduction. All four treat the denoising trajectory as a black box, assigning uniform credit across steps. DACA-GRPO is the first to exploit trajectory-level signals for credit assignment.

Temporal credit assignment is a classical challenge in reinforcement learning (Sutton and Barto, 2018). In the autoregressive setting, per-token reward models (Lightman et al., 2024; Zhu et al., 2025) and process reward models (Uesato et al., 2022) provide step-level supervision but require training additional reward models or collecting extra annotations. DPS addresses the same challenge by exploiting a structural property of diffusion models: intermediate predictions are already computed during generation but usually discarded. Concurrently, DyLLM (Lee et al., 2026) observes that not all token positions contribute equally across denoising steps and identifies *salient* positions via attention-context similarity to accelerate inference. Both methods mine signals from the denoising trajectory, but to different ends: DyLLM uses attention-based saliency to accelerate inference, while DPS uses token-level prediction confidence to improve *training* via credit assignment.

SML applies a different principle to masked-token likelihood estimation: instead of stratifying the masking *ratio* (as in DiffuCoder’s antithetic timesteps (Gong et al., 2025)) or using deterministic quadrature over time (as in GDPO’s SDMC (Rojas et al., 2026)), we stratify token *positions*—masking one stratum at a time to provide partial context, targeting mean-field estimation error rather than sampling *variance*.

3 Background

Masked diffusion language models (Sahoo et al., 2024; Nie et al., 2026) define a forward process that progressively masks tokens and a reverse process that denoises them. Given a clean sequence $\mathbf{x}_0 = (x_1, \dots, x_L)$, the forward process produces a noisy sequence \mathbf{x}_t at timestep $t \in [0, 1]$ by independently replacing each token with [MASK] with probability t . The reverse (generative) process starts with a fully masked sequence \mathbf{x}_1 and iteratively predicts and reveals tokens until reaching \mathbf{x}_0 . At each denoising step t , the model p_θ predicts a distribution $p_\theta(x_i | \mathbf{x}_t)$ over all vocabulary tokens for every masked position $i \in \mathcal{M}_t$, where $\mathcal{M}_t = \{i : x_{t,i} = \text{[MASK]}\}$. A fixed number k of masked positions are then unmasked by selecting positions and tokens with the highest model confidence. In particular, predictions are made for *all* masked positions but most are discarded. These “wasted” predictions form the basis of our DPS mechanism.

GRPO for diffusion language models (Shao et al., 2024) generates a group of G candidate responses $\{y^{(g)}\}_{g=1}^G$ for each prompt, computes rewards $\{r^{(g)}\}$, and defines group-relative advantages using the group mean μ_r and standard deviation σ_r :

$$A^{(g)} = \frac{r^{(g)} - \mu_r}{\sigma_r}. \quad (3.1)$$

Diffu-GRPO (Zhao et al., 2025) adapts GRPO to dLLMs using a per-token PPO-clipped surrogate objective with per-token likelihood ratio $\rho_i(\theta) = p_\theta(x_i | \mathbf{m})/p_{\theta_{\text{old}}}(x_i | \mathbf{m})$, computed with all completion tokens masked (\mathbf{m}):

$$\mathcal{L}_{\text{d1}} = -\mathbb{E} [\min(\rho_i(\theta)A, \text{clip}(\rho_i(\theta), 1 - \epsilon, 1 + \epsilon)A)]. \quad (3.2)$$

wd1 (Tang et al., 2026) proposes a ratio-free alternative with explicit positive and negative sample reinforcement, using normalized advantage weights $\hat{A}_+^{(g)} = \text{softmax}(A^{(g)})$ and $\hat{A}_-^{(g)} = \text{softmax}(-A^{(g)})$:

$$\mathcal{L}_{\text{wd1}} = - \underbrace{\sum_{g:A^{(g)}>0} \hat{A}_+^{(g)} \log p_\theta(y^{(g)})}_{\text{PSR: amplify correct}} + \underbrace{\sum_{g:A^{(g)}<0} \hat{A}_-^{(g)} \log p_\theta(y^{(g)})}_{\text{NSR: suppress incorrect}}. \quad (3.3)$$

GDPO (Rojas et al., 2026) operates at the *sequence level*, using the evidence lower bound (ELBO) as a surrogate for $\log p_\theta(y)$:

$$\mathcal{L}_{\text{ELBO}}(y | q) = \mathbb{E}_{t \sim \mathcal{U}[0,1]} \mathbb{E}_{y_t \sim \pi_t(\cdot | y)} \left[\frac{1}{t} \sum_{i=1}^L \mathbf{1}[y_{t,i} = \mathbb{M}] \log \pi_\theta(y_i | y_t, q) \right]. \quad (3.4)$$

To reduce variance, GDPO introduces Semi-deterministic Monte Carlo (SDMC): N fixed quadrature points over t with random mask sampling. The loss uses sequence-level importance ratios $r_g = \mathcal{L}_{\text{ELBO}}^\theta(y_g | q) / \mathcal{L}_{\text{ELBO}}^{\theta_{\text{old}}}(y_g | q)$ and unnormalized advantages $A_g = r_g - \text{mean}(r_1, \dots, r_G)$:

$$\mathcal{L}_{\text{GDPO}}(\theta) = -\frac{1}{G} \sum_{g=1}^G \frac{1}{|y_g|} \min(r_g \cdot A_g, \text{clip}(r_g, 1 - \epsilon, 1 + \epsilon) \cdot A_g) + \beta \text{KL}(\pi_\theta \| \pi_{\text{ref}}). \quad (3.5)$$

Masked-token log-likelihood. All three methods require estimating $\log p_\theta(y)$ for each completion. In dLLMs, this is typically approximated by sampling a random masking ratio $t \sim \mathcal{U}(0, 1)$, constructing a masked version \mathbf{x}_t , and computing:

$$\log p_\theta(y) \approx \frac{1}{|\mathcal{M}_t|} \sum_{i \in \mathcal{M}_t} \log p_\theta(x_i | \mathbf{x}_t). \quad (3.6)$$

Here $p_\theta(x_i | \mathbf{x}_t)$ is obtained from the model’s output logits at position i via softmax—each per-token log-probability is exact; the approximation arises from the mean-field factorization into independent per-token terms. d1 and wd1 use this single-sample estimate directly, incurring high variance and mean-field bias (all tokens masked, zero inter-token context). GDPO reduces variance via deterministic quadrature over t , but the per-point estimates remain subject to the same bias. SML addresses the mean-field bias by predicting each token with $(K-1)/K$ of the sequence as context.

4 Weaknesses of current approaches

Weakness 1: No Temporal Credit Assignment In autoregressive models, the sequential generation process naturally induces a form of credit assignment: each token’s probability is conditioned on all preceding tokens, and per-token rewards or advantages can be assigned based on position. Diffusion models lack this structure. All tokens are predicted simultaneously at each step, and the RL loss (equations (3.2) and (3.3)) assigns a single scalar advantage $A^{(g)}$ to the *entire* completion. Denoising steps vary dramatically in importance: some involve decisive transitions where the model commits to key structural choices, while others are routine fill-in with minimal belief change. Standard methods assign equal weight to all steps and discard the intermediate predictions entirely. More specifically, uniform weighting under-credits *decisive steps* that involve major belief changes—committing to key tokens such as operators in math or control flow in code—while over-crediting *routine steps* with minimal belief change. It also over-punishes *self-correcting steps* where the model doubts an incorrect answer, despite already moving toward the right solution. The result is inefficient gradient updates that fail to concentrate learning on the steps that matter most.

Weakness 2: Biased and High-Variance Likelihood Estimates All three base methods require estimating $\log p_\theta(y)$ for each completion. The standard approach (equation (3.6)) masks *all* completion tokens and predicts them from zero context, treating tokens as independent. This introduces *systematic bias*: predicting without any context is fundamentally harder, adding errors to the log likelihood estimates. It also introduces *high variance*: a single random masking pattern may over- or under-represent the typical difficulty of predicting y , producing noisy gradients.

5 Method

We present DACA-GRPO, which addresses both weaknesses through two complementary mechanisms: *Denoising Progress Scores* and *Stratified Masking Likelihood*.

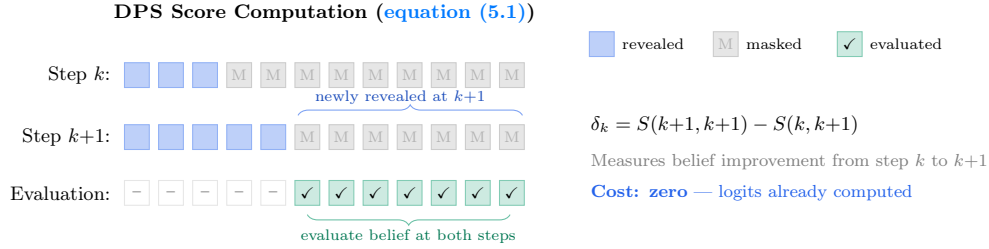


Figure 2 DPS score computation. We quantify the change in model beliefs by computing the difference δ_k in model predictions on positions masked in the current and the following step. DPS uses the logits computed naturally during generation and requires no extra forward passes.

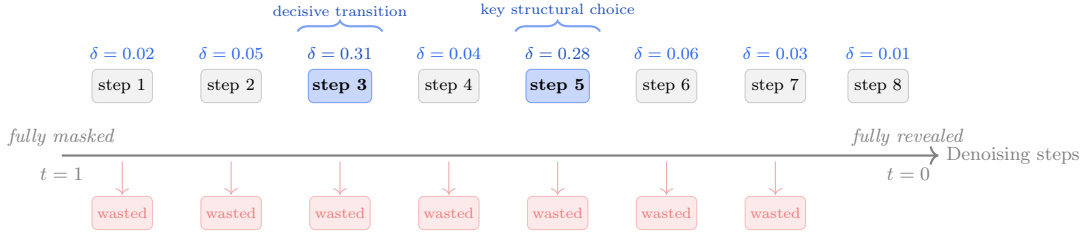


Figure 3 Illustration of Weakness 1. During generation, dLLMs perform many denoising steps of varying importance. Steps 3 and 5 involve decisive transitions (large δ), while others are routine. Standard methods assign equal credit to all steps and discard intermediate predictions.

5.1 Denoising progress scores (DPS)

At each denoising step, the model predicts token distributions for all masked positions, but only unmask a few. The predictions at still-masked positions reveal how well the model “understands” the emerging sequence—and how much that understanding changes between steps provides a natural measure of step importance.

Formally, let $\mathbf{x}_0, \mathbf{x}_1, \dots, \mathbf{x}_T$ denote the denoising trajectory and $\mathcal{M}_T \subset \mathcal{M}_{T-1} \subset \dots \subset \mathcal{M}_0$ the family of masked positions (\mathbf{x}_0 fully masked, \mathbf{x}_T fully revealed). We define $S(k, j)$ as the average log-probability under the model at step k over the positions in \mathcal{M}_j :

$$S(k, j) = \frac{1}{|\mathcal{M}_j|} \sum_{i \in \mathcal{M}_j} \log p_{\theta}(x_i^* | \mathbf{x}_k), \quad (5.1)$$

where x_i^* is the final token at position i in the model’s own generated completion, i.e., the token the model itself selected during the rollout, not an external label. The *denoising progress delta* at step k measures the belief improvement when transitioning from step k to $k+1$:

$$\delta_k := S(k+1, k+1) - S(k, k+1) \quad (5.2)$$

Both scores are evaluated on the same set of positions \mathcal{M}_{k+1} (i.e., those still masked at the next step), so the difference isolates the effect of the newly revealed tokens (figure 2). A large positive δ indicates that revealing tokens at step $k+1$ substantially improved the model’s understanding (i.e., an important denoising step). A small or negative δ indicates minimal or confused progress (figure 3).

DPS requires no additional forward passes. At each denoising step, the model already computes logits for all masked positions; DPS reuses the log-probabilities at still-masked positions, values that would otherwise be discarded. The only overhead is one scalar per recorded step per sample (<1% wall-clock; appendix C.6).

Raw deltas vary in scale across denoising steps due to the non-stationary nature of the denoising process (early steps have little context and small deltas; late steps have rich context and larger deltas). Therefore,

we apply *per-step* z-score normalization across the batch:

$$\bar{\delta}_k = \frac{\delta_k - \mu_k}{\sigma_k + \epsilon}, \quad (5.3)$$

where μ_k and σ_k are the batch mean and standard deviation of δ_k . This ensures fair credit assignment across the entire denoising timeline: an “impressive” early-step delta and an “impressive” late-step delta receive comparable normalized values, despite different magnitudes. We compared four alternatives and found that per-step exceeds the baseline across all stride configurations (Appendix C.2).

Per-token weight modulation. Each token in the final sequence is “born” at the denoising step where it was unmasked. We track birth step and define the *DPS-modulated per-token advantage*:

$$\tilde{A}_i^{(g)} = A^{(g)} \cdot (1 + \lambda \cdot \bar{\delta}_{\text{birth}(i)}), \quad (5.4)$$

where $\lambda > 0$ controls modulation strength. The factor $\omega_i = 1 + \lambda \cdot \bar{\delta}_{\text{birth}(i)}$ amplifies or attenuates the learning signal based on step importance. For negative-advantage samples, the sign of $\bar{\delta}$ provides directional credit: positive values increase punishment (confident progress toward the wrong answer), negative ones decrease it (hesitation or self-correction).

DPS implementation requires two design choices: (1) tokens unmasked at the final recorded denoising step have no following step to compute a delta against, so we extrapolate $\delta_T = \delta_{T-1}$; (2) we record snapshots with a stride s , trading credit granularity for signal-to-noise. Both choices are robust: extrapolation outperforms four alternatives, and every stride $s \in \{1, 2, 4, 8, 16, 32\}$ exceeds the baseline under our default settings. Ablations and detailed discussion in appendices B and C.1.

5.2 Stratified masking likelihood (SML)

Log-likelihood estimates used by all three base methods mask *all* completion tokens and predict them from zero inter-token context. This mean-field approximation introduces error (equations (3.2), (3.3) and (3.5)). To mitigate this, we propose a stratified estimator that uses K forward passes. We partition the N output token positions o_1, \dots, o_N of completion y into K disjoint strata $\mathcal{S}_1, \dots, \mathcal{S}_K$ of roughly equal size. For each stratum \mathcal{S}_k , we mask *only* the positions in \mathcal{S}_k while keeping all other output tokens visible, and compute per-token log-probability for each masked position $n \in \mathcal{S}_k$. Summing the token-level log-probabilities across all strata gives the sequence-level SML estimate:

$$\log p_\theta^{\text{SML}}(o|q) = \sum_{k=1}^K \sum_{n \in \mathcal{S}_k} \log p_\theta(o_n | o_{\setminus \mathcal{S}_k}, q), \quad (5.5)$$

where $o_{\setminus \mathcal{S}_k}$ denotes the output sequence with only stratum \mathcal{S}_k replaced by mask tokens. Each token is predicted with $(K-1)/K$ of the sequence as visible context, forming a tunable spectrum: $K=1$ places all tokens in a single stratum, recovering the fully-masked estimate of equation (3.6); $K=N$ gives each token its own stratum, recovering the pseudo-log-likelihood where every token sees all others (figure 4). We hypothesize that this method of approximating the log probabilities reduces the estimation errors in mean-field based methods such as d1 and we verify this hypothesis empirically in Section 6. SML targets the *bias* component of mean-field error—complementary to variance-reduction methods like GDPO’s SDMC.

5.3 SML integration

Integrating SML into the training loss depends on whether the base method uses a clipped importance ratio.

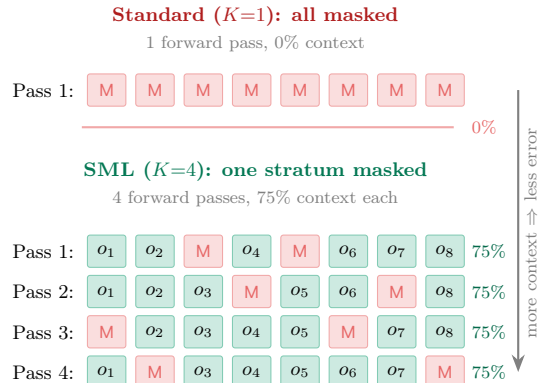


Figure 4 Stratified Masking Likelihood. Standard estimation ($K=1$) masks all tokens with zero context. SML ($K=4$) masks one stratum per pass, giving each token 75% context.

Algorithm 1 DACA-GRPO

Require: Policy π_θ , reward R , stride s , modulation strength λ , strata K

```
1: for each training step do
2:   Generate  $G$  completions; cache logits at still-masked positions every  $s$  steps
3:   Compute rewards and group-relative advantages  $A^{(g)}$ 
4:   DPS: compute progress deltas  $\delta_k$  from cached logits equations (5.1) and (5.2)
5:   DPS: per-token advantages  $\tilde{A}_i^{(g)} \leftarrow A^{(g)} \cdot (1 + \lambda \cdot \bar{\delta}_{\text{birth}(i)})$  equations (5.3) and (5.4)
6:   for each inner iteration do
7:     SML: compute  $K$ -stratum likelihood  $\log p_\theta^{\text{SML}}(y)$  equation (5.5)
8:     Compute  $\mathcal{L}_{\text{DACA}}$  using  $\tilde{A}_i^{(g)}$  and SML likelihood equation (5.9) or equation (5.10)
9:     Update  $\theta$  via gradient descent
10:  end for
11: end for
```

Ratio-Free Methods like wd1 optimize log-probabilities directly without importance ratios or trust regions. Adding an SML-based likelihood term is therefore straightforward—both losses operate on $\log p_\theta$ and their gradients compose without conflict:

$$\mathcal{L}_{\text{DACA-wd1}} = \mathcal{L}_{\text{wd1}} - \frac{\eta}{G} \sum_{g=1}^G \log p_\theta^{\text{SML}}(y^{(g)}), \quad (5.6)$$

where η controls the SML loss strength. The base loss handles reward-driven credit assignment (amplifying correct answers, suppressing incorrect ones), while the SML term provides a complementary signal that improves token-prediction quality under richer context.

Ratio-Based Methods like d1 and GDPO (equations (3.2) and (3.5)) cannot accept an additive SML loss as it destabilizes training: its gradient bypasses the PPO clip, resulting in training collapse. Instead, we incorporate SML *inside* the importance ratio at token level. For each output position i , let $k(i)$ denote the stratum containing position i . We form an enriched per-token log-probability by averaging two views—the fully-masked prediction and the stratum prediction:

$$\hat{\ell}_{\theta,i} = \frac{1}{2} \left[\log p_\theta(o_i | \mathbf{m}, q) + \log p_\theta(o_i | o_{\setminus \mathcal{S}_{k(i)}}, q) \right], \quad (5.7)$$

where \mathbf{m} denotes the fully-masked completion (the standard estimate from equation (3.6)) and $o_{\setminus \mathcal{S}_{k(i)}}$ denotes the completion with only stratum $\mathcal{S}_{k(i)}$ masked. This yields a per-token importance ratio:

$$\rho_i^{\text{SML}} := \exp\left(\hat{\ell}_{\theta,i} - \hat{\ell}_{\theta_{\text{old}},i}\right), \quad (5.8)$$

which replaces the standard per-token ratio in the clipped surrogate. Each token’s enriched log-probability blends the fully-masked view (matching the generation regime) with its stratified view (reducing estimation errors). The trust region is preserved by construction ($\rho_i^{\text{SML}}(\theta_{\text{old}}) = 1$); $\hat{\ell}_{\theta_{\text{old}},i}$ is computed once and cached. No hyperparameters beyond K are introduced. SML adds K forward passes during loss computation—negligible relative to the generation phase that dominates each training step (see appendix C.6).

5.4 DACA-GRPO: combining DPS and SML

DPS and SML can be applied separately or jointly, as they modify two independent inputs to the loss: DPS modulates the per-token advantage while SML improves the likelihood estimate. For ratio-free methods, the **combined loss** becomes:

$$\mathcal{L}_{\text{DACA}} = \mathcal{L}_{\text{wd1}}\left(\tilde{A}_i^{(g)}\right) - \frac{\eta}{G} \sum_{g=1}^G \log p_\theta^{\text{SML}}(y^{(g)}), \quad (5.9)$$

where the first term is the wd1 loss, but with DPS per-token advantages, and the second is the SML loss. For ratio-based methods, SML enters inside the importance ratio and DPS modulates the per-token advantages:

$$\mathcal{L}_{\text{DACA}} = -\mathbb{E} \left[\min \left(\rho_i^{\text{SML}} \cdot \tilde{A}_i^{(g)}, \text{clip}(\rho_i^{\text{SML}}, 1-\epsilon, 1+\epsilon) \cdot \tilde{A}_i^{(g)} \right) \right]. \quad (5.10)$$

algorithm 1 gives the complete procedure. The key structural property is that DPS weights are computed once per training step during generation (at zero additional cost) and reused across all inner iterations, while SML forward passes occur within each inner iteration during loss computation.

6 Experiments

Setup. We use LLaDA-8B-Instruct (Nie et al., 2026) as the base dLLM, consistent with prior work (Zhao et al., 2025; Tang et al., 2026). We evaluate DACA-GRPO on top of three GRPO variants: Diffu-GRPO (Zhao et al., 2025) (PPO-clipped surrogate with importance ratios), wd1 (Tang et al., 2026) (ratio-free weighted log-likelihood), and GDPO (Rojas et al., 2026) (token-level diffusion policy optimization).

We evaluate on seven benchmarks: MATH-500 (Hendrycks et al., 2021) and GSM8K (Cobbe et al., 2021) for mathematical reasoning; MBPP (Austin et al., 2021) and HumanEval (Chen et al., 2021) for code generation; Countdown and Sudoku for constraint satisfaction; and JSON schema adherence for constrained generation. The full DACA-GRPO framework (DPS + SML) is applied to math, code tasks, and JSON generation (tables 1 and 11) as well as for constrained generation; for constraint satisfaction, only DPS is applied (table 2). We evaluate at generation lengths 128, 256, and 512 with proportionally scaled diffusion steps to maintain consistency with Zhao et al. (2025); Tang et al. (2026). For Sudoku, we report accuracy per-empty-cell following Tang et al. (2026). appendices A and C contain more details and analyses.

Table 1 Accuracy (%) on math reasoning and code generation tasks (pass@1) by generation length.

| Method | MATH-500 | | | GSM8K | | | MBPP | | | HumanEval | | |
|----------------|-------------|-------------|-------------|-------------|-------------|-------------|-------------|-------------|-------------|-------------|-------------|-------------|
| | 128 | 256 | 512 | 128 | 256 | 512 | 128 | 256 | 512 | 128 | 256 | 512 |
| LLaDA-8B-Inst. | 26.0 | 32.4 | 36.2 | 68.7 | 76.7 | 78.2 | 35.8 | 42.6 | 45.2 | 17.1 | 26.2 | 34.2 |
| Diffu-GRPO | 31.8 | 37.1 | 39.2 | 72.1 | 79.2 | 79.8 | 41.7 | 44.9 | 44.2 | 19.8 | 32.3 | 35.4 |
| + DPS | 33.5 | 37.5 | 40.2 | 74.0 | 80.8 | 80.9 | 47.0 | 46.5 | 45.6 | 22.9 | 32.8 | 36.5 |
| + SML | 34.3 | 38.3 | 40.5 | 74.6 | 81.6 | 81.5 | 44.4 | 47.5 | 48.6 | 26.6 | 36.5 | 40.6 |
| + DACA-GRPO | 35.4 | 38.8 | 40.5 | 74.6 | 81.6 | 81.5 | 45.4 | 48.1 | 50.5 | 25.5 | 35.4 | 40.1 |
| wd1 | 32.6 | 36.7 | 39.6 | 70.5 | 80.6 | 80.7 | 45.4 | 45.8 | 45.8 | 21.9 | 34.9 | 37.5 |
| + DPS | 33.5 | 39.8 | 40.9 | 72.8 | 81.6 | 81.6 | 46.1 | 47.5 | 47.5 | 25.0 | 36.5 | 40.0 |
| + SML | 34.3 | 39.4 | 41.5 | 74.9 | 81.9 | 82.0 | 45.8 | 47.2 | 47.2 | 25.5 | 34.9 | 39.1 |
| + DACA-GRPO | 35.6 | 40.2 | 41.3 | 76.1 | 82.1 | 82.1 | 45.4 | 48.6 | 50.7 | 25.0 | 35.9 | 40.1 |
| GDPO | 33.9 | 36.9 | 40.7 | 73.6 | 80.6 | 80.0 | 38.9 | 45.1 | 46.1 | 18.8 | 37.0 | 37.0 |
| + DPS | 34.9 | 39.0 | 40.7 | 75.1 | 80.6 | 82.8 | 40.7 | 47.7 | 48.2 | 21.9 | 35.9 | 40.0 |
| + SML | 34.5 | 39.0 | 40.2 | 74.0 | 80.6 | 80.6 | 45.8 | 47.5 | 50.0 | 25.5 | 36.5 | 40.6 |
| + DACA-GRPO | 35.2 | 38.6 | 41.7 | 74.3 | 81.6 | 82.0 | 46.3 | 48.1 | 49.5 | 25.0 | 37.0 | 41.1 |

Main Results. table 1 presents mathematical reasoning (MATH-500, GSM8K) and code generation results (MBPP, HumanEval). Three patterns emerge.

DPS and SML are complementary. DACA-GRPO achieves the best or tied-best average improvement in 9 of 12 method–benchmark combinations. From table 1 we see that SML and DPS are complementary; both methods lead to increases and together (with DACA-GRPO) we see near additive results. For example, on wd1 MBPP, DPS alone adds +1.4pp and SML alone adds +1.1pp, but DACA-GRPO adds +2.6pp—more than either component and close to their sum. This confirms DACA-GRPO is usually the best choice.

The two mechanisms target different regimes. DPS contributes most at short generation lengths, where each denoising step resolves a larger fraction of the output and the distinction between decisive and routine steps is sharpest (e.g., +5.3pp on MBPP at $L=128$ with d1). SML contributes most at long generation

lengths, where inter-token dependencies are stronger and the mean-field bias is more severe (e.g., +4.4pp on MBPP at $L=512$ with d1; +5.2pp on HumanEval at $L=512$ with d1). DACA-GRPO captures both effects, achieving the highest MBPP accuracy at $L=512$ across all three base methods (50.5, 50.7, and 49.5 respectively).

Improvements are consistent across base methods. Each individual component improves nearly every method–benchmark combination regardless of whether the base method is ratio-based (d1, GDPO) or ratio-free (wd1), and regardless of whether it operates at the token level (d1, wd1) or sequence level (GDPO). This validates the plug-and-play design: DPS and SML address upstream weaknesses in the training signal that are shared across loss formulations.

SML Applicability: Task Structure and Output Length. We apply SML only to long-form tasks (MATH-500, GSM8K, MBPP, HumanEval) and excluded from constraint satisfaction (Countdown, Sudoku) due to a distributional mismatch. SML evaluates each token with $(K-1)/K$ visible context (75% for $K=4$), whereas generation starts fully masked. For short, tightly constrained outputs (~ 7 empty Sudoku cells, 10–15 Countdown tokens), 75% context nearly determines the answer via constraint propagation, driving the model toward trivial gap-filling that fails at generation.

Constraint satisfaction analysis. DPS delivers the most dramatic improvements on Sudoku, where wd1 + DPS improves per-cell accuracy by +26–36pp (table 2)—consistent with the task’s tight inter-cell dependencies, which make decisive denoising steps especially impactful. The jump reflects a qualitative shift: wd1’s per-cell accuracy at $L=512$ rises from 34.6% to 70.9%, crossing from unreliable to reliable. On Countdown, DPS improves d1 and wd1 consistently (+1.2–10.4pp) but shows a small degradation on GDPO at $L=128$ (−2.4pp), likely because GDPO’s stronger baseline leaves less headroom.

JSON generation. DPS improves schema adherence for all three base methods (Figure 1). The task is non-trivial even after RL post-training: the strongest base method (wd1 at $L=512$) reaches only 72.57% schema adherence on GITHUB-MEDIUM, reflecting the difficulty of generating nested structures that fully conform to a target schema. Combining both components amplifies the effect: DACA-GRPO achieves the highest schema adherence on wd1 (+5.90pp, reaching 78.47%) and GDPO (+3.82pp), with DPS and SML contributing comparably on wd1 alone (+3.47pp and +3.82pp). d1 is the lone exception: DPS alone (+4.52pp) narrowly beats DACA-GRPO (+4.17pp), suggesting mild interference between the two components. Despite JSON’s rigid schema structure, SML is effective here—unlike on Sudoku and Countdown—because outputs at $L=512$ are long enough that partial-mask context does not trivially determine the remaining tokens. This sharpens SML’s applicability boundary as length-driven rather than structure-driven; see appendix C.7 for the full table and analysis.

Table 2 Constraint satisfaction (DPS only). Accuracy (%) on Countdown and Sudoku. Sudoku uses per-cell accuracy (Tang et al., 2026).

| Method | Countdown | | | Sudoku | | |
|----------------|-------------|-------------|-------------|-------------|-------------|-------------|
| | 128 | 256 | 512 | 128 | 256 | 512 |
| LLaDA-8B-Inst. | 20.7 | 19.5 | 16.0 | 11.7 | 6.7 | 5.5 |
| Diffu-GRPO | 50.0 | 50.3 | 47.9 | 25.9 | 26.2 | 26.3 |
| + DPS | 57.6 | 55.2 | 53.8 | 26.8 | 29.2 | 37.5 |
| wd1 | 53.1 | 53.1 | 47.9 | 51.4 | 40.5 | 34.6 |
| + DPS | 54.3 | 56.9 | 58.3 | 77.6 | 76.1 | 70.9 |
| GDPO | 62.5 | 69.4 | 74.7 | 26.1 | 26.2 | 25.8 |
| + DPS | 60.1 | 70.2 | 76.8 | 38.9 | 50.0 | 37.5 |

7 Discussion and conclusion

We presented DACA-GRPO, a plug-and-play framework that brings temporal credit assignment and improved likelihood estimation to any GRPO-style dLLM trainer, with consistent improvement across seven benchmarks and three base methods.

The most striking result is that “wasted” intermediate predictions—logits that existing methods compute and discard at every denoising step—contain enough signal to meaningfully improve training. DPS exploits this signal at near-zero cost, and the dramatic Sudoku gains (+26–36pp) suggest that structured tasks with tight inter-token dependencies are especially under-served by uniform credit assignment. More broadly, the fact

that a simple per-step importance measure transfers across ratio-based and ratio-free losses, across math, code, and constraint satisfaction domains, and across short and long generation lengths indicates that the missing credit-assignment structure is a shared bottleneck in current dLLM RL pipelines—not an artifact of any single loss formulation.

SML complements DPS for long-form tasks where mean-field bias is most severe, but its value diminishes when the base method already diversifies likelihood views (as with GDPO’s SDMC). This points to a practical guideline: DPS is a universal add-on, while SML should be prioritized for methods and tasks where likelihood quality is the binding constraint.

Limitations. SML is not applicable to short, tightly constrained outputs, where the distributional mismatch between partial-mask training and fully-masked generation causes mode collapse; developing a likelihood regularizer effective across all output lengths remains open.

Future directions. Adaptive stride selection—adjusting recording frequency based on observed delta magnitudes—could improve the signal-to-noise tradeoff without manual tuning. Finally, SML’s stratified estimation principle may extend beyond RL to the pre-training objective itself, where the same mean-field bias affects the masked diffusion loss.

References

- Jacob Austin, Augustus Odena, Maxwell Nye, Maarten Bosma, Henryk Michalewski, David Dohan, Ellen Jiang, Carrie Cai, Michael Terry, Quoc Le, and Charles Sutton. Program synthesis with large language models, 2021. URL <https://arxiv.org/abs/2108.07732>.
- Kevin Black, Michael Janner, Yilun Du, Ilya Kostrikov, and Sergey Levine. Training diffusion models with reinforcement learning. In *The Twelfth International Conference on Learning Representations*, 2024. URL <https://openreview.net/forum?id=YCWjhGrJFD>.
- Mark Chen, Jerry Tworek, Heewoo Jun, Qiming Yuan, Henrique Ponde de Oliveira Pinto, Jared Kaplan, Harri Edwards, Yuri Burda, Nicholas Joseph, Greg Brockman, Alex Ray, Raul Puri, Gretchen Krueger, Michael Petrov, Heidy Khlaaf, Girish Sastry, Pamela Mishkin, Brooke Chan, Scott Gray, Nick Ryder, Mikhail Pavlov, Alethea Power, Lukasz Kaiser, Mohammad Bavarian, Clemens Winter, Philippe Tillet, Felipe Petroski Such, Dave Cummings, Matthias Plappert, Fotios Chantzis, Elizabeth Barnes, Ariel Herbert-Voss, William Hebgen Guss, Alex Nichol, Alex Paino, Nikolas Tezak, Jie Tang, Igor Babuschkin, Suchir Balaji, Shantanu Jain, William Saunders, Christopher Hesse, Andrew N. Carr, Jan Leike, Josh Achiam, Vedant Misra, Evan Morikawa, Alec Radford, Matthew Knight, Miles Brundage, Mira Murati, Katie Mayer, Peter Welinder, Bob McGrew, Dario Amodei, Sam McCandlish, Ilya Sutskever, and Wojciech Zaremba. Evaluating large language models trained on code, 2021. URL <https://arxiv.org/abs/2107.03374>.
- Karl Cobbe, Vineet Kosaraju, Mohammad Bavarian, Mark Chen, Heewoo Jun, Lukasz Kaiser, Matthias Plappert, Jerry Tworek, Jacob Hilton, Reiichiro Nakano, Christopher Hesse, and John Schulman. Training verifiers to solve math word problems, 2021. URL <https://arxiv.org/abs/2110.14168>.
- Di Feng, Kaixin Ma, Feng Nan, Haofeng Chen, Bohan Zhai, David Griffiths, Mingfei Gao, Zhe Gan, Eshan Verma, Yinfei Yang, Zhifeng Chen, and Afshin Dehghan. So-bench: A structural output evaluation of multimodal llms, 2026. URL <https://arxiv.org/abs/2511.21750>.
- Saibo Geng, Hudson Cooper, Michał Moskal, Samuel Jenkins, Julian Berman, Nathan Ranchin, Robert West, Eric Horvitz, and Harsha Nori. Jsonschemabench: A rigorous benchmark of structured outputs for language models, 2025. URL <https://arxiv.org/abs/2501.10868>.
- Shansan Gong, Ruixiang Zhang, Huangjie Zheng, Jiatao Gu, Navdeep Jaitly, Lingpeng Kong, and Yizhe Zhang. Diffu-coder: Understanding and improving masked diffusion models for code generation. *arXiv preprint arXiv:2506.20639*, 2025. URL <https://arxiv.org/abs/2506.20639>.
- Daya Guo, Dejian Yang, Haowei Zhang, Junxiao Song, Peiyi Wang, Qihao Zhu, Runxin Xu, Ruoyu Zhang, Shirong Ma, Xiao Bi, Xiaokang Zhang, Xingkai Yu, Yu Wu, Z. F. Wu, Zhibin Gou, Zhihong Shao, Zhuoshu Li, Ziyi Gao, Aixin Liu, Bing Xue, Bingxuan Wang, Bochao Wu, Bei Feng, Chengda Lu, Chenggang Zhao, Chengqi Deng, Chong Ruan, Damai Dai, Deli Chen, Dongjie Ji, Erhang Li, Fangyun Lin, Fucong Dai, Fuli Luo, Guangbo Hao, Guanting Chen, Guowei Li, H. Zhang, Hanwei Xu, Honghui Ding, Huazuo Gao, Hui Qu, Hui Li, Jianzhong Guo, Jiashi Li, Jingchang Chen, Jingyang Yuan, Jinhao Tu, Junjie Qiu, Junlong Li, J. L. Cai, Jiaqi Ni, Jian Liang, Jin Chen, Kai

- Dong, Kai Hu, Kaichao You, Kaige Gao, Kang Guan, Kexin Huang, Kuai Yu, Lean Wang, Lecong Zhang, Liang Zhao, Litong Wang, Liyue Zhang, Lei Xu, Leyi Xia, Mingchuan Zhang, Minghua Zhang, Minghui Tang, Mingxu Zhou, Meng Li, Miaojun Wang, Mingming Li, Ning Tian, Panpan Huang, Peng Zhang, Qiancheng Wang, Qinyu Chen, Qiushi Du, Ruiqi Ge, Ruisong Zhang, Ruizhe Pan, Runji Wang, R. J. Chen, R. L. Jin, Ruyi Chen, Shanghao Lu, Shangyan Zhou, Shanhuang Chen, Shengfeng Ye, Shiyu Wang, Shuiping Yu, Shunfeng Zhou, Shuting Pan, S. S. Li, Shuang Zhou, Shaoqing Wu, Tao Yun, Tian Pei, Tianyu Sun, T. Wang, Wangding Zeng, Wen Liu, Wenfeng Liang, Wenjun Gao, Wenqin Yu, Wentao Zhang, W. L. Xiao, Wei An, Xiaodong Liu, Xiaohan Wang, Xiaokang Chen, Xiaotao Nie, Xin Cheng, Xin Liu, Xin Xie, Xingchao Liu, Xinyu Yang, Xinyuan Li, Xuecheng Su, Xuheng Lin, X. Q. Li, Xiangyue Jin, Xiaojin Shen, Xiaosha Chen, Xiaowen Sun, Xiaoxiang Wang, Xinnan Song, Xinyi Zhou, Xianzu Wang, Xinxia Shan, Y. K. Li, Y. Q. Wang, Y. X. Wei, Yang Zhang, Yanhong Xu, Yao Li, Yao Zhao, Yaofeng Sun, Yaohui Wang, Yi Yu, Yichao Zhang, Yifan Shi, Yiliang Xiong, Ying He, Yishi Piao, Yisong Wang, Yixuan Tan, Yiyang Ma, Yiyuan Liu, Yongqiang Guo, Yuan Ou, Yuduan Wang, Yue Gong, Yuheng Zou, Yujia He, Yunfan Xiong, Yuxiang Luo, Yuxiang You, Yuxuan Liu, Yuyang Zhou, Y. X. Zhu, Yanping Huang, Yaohui Li, Yi Zheng, Yuchen Zhu, Yunxian Ma, Ying Tang, Yukun Zha, Yuting Yan, Z. Z. Ren, Zehui Ren, Zhangli Sha, Zhe Fu, Zhean Xu, Zhenda Xie, Zhengyan Zhang, Zhewen Hao, Zhicheng Ma, Zhigang Yan, Zhiyu Wu, Zihui Gu, Zijia Zhu, Zijun Liu, Zilin Li, Ziwei Xie, Ziyang Song, Zizheng Pan, Zhen Huang, Zhipeng Xu, Zhongyu Zhang, and Zhen Zhang. Deepseek-r1 incentivizes reasoning in llms through reinforcement learning. *Nature*, 645(8081):633–638, September 2025. ISSN 1476-4687. doi: 10.1038/s41586-025-09422-z. URL <http://dx.doi.org/10.1038/s41586-025-09422-z>.
- Dan Hendrycks, Collin Burns, Saurav Kadavath, Akul Arora, Steven Basart, Eric Tang, Dawn Song, and Jacob Steinhardt. Measuring mathematical problem solving with the MATH dataset. In *Thirty-fifth Conference on Neural Information Processing Systems Datasets and Benchmarks Track (Round 2)*, 2021. URL <https://openreview.net/forum?id=7Bywt2mQsCe>.
- Inception Labs, Samar Khanna, Siddhant Kharbanda, Shufan Li, Harshit Varma, Eric Wang, Sawyer Birnbaum, Ziyang Luo, Yanis Miraoui, Akash Palrecha, Stefano Ermon, Aditya Grover, and Volodymyr Kuleshov. Mercury: Ultra-fast language models based on diffusion, 2025. URL <https://arxiv.org/abs/2506.17298>.
- Younjoo Lee, Junghoo Lee, Seungkyun Dan, Jaiyoung Park, and Jung Ho Ahn. Dyllm: Efficient diffusion llm inference via saliency-based token selection and partial attention, 2026. URL <https://arxiv.org/abs/2603.08026>.
- Hunter Lightman, Vineet Kosaraju, Yuri Burda, Harrison Edwards, Bowen Baker, Teddy Lee, Jan Leike, John Schulman, Ilya Sutskever, and Karl Cobbe. Let’s verify step by step. In *The Twelfth International Conference on Learning Representations*, 2024. URL <https://openreview.net/forum?id=v8LOpN6EOI>.
- Zichen Liu, Changyu Chen, Wenjun Li, Penghui Qi, Tianyu Pang, Chao Du, Wee Sun Lee, and Min Lin. Understanding r1-zero-like training: A critical perspective, 2025. URL <https://arxiv.org/abs/2503.20783>.
- Aaron Lou, Chenlin Meng, and Stefano Ermon. Discrete diffusion modeling by estimating the ratios of the data distribution. In *Proceedings of the 41st International Conference on Machine Learning*, ICML’24. JMLR.org, 2024.
- Amin Karimi Monsefi, Nikhil Bhendawade, Manuel Rafael Ciosici, Dominic Culver, Yizhe Zhang, and Irina Belousova. FS-DFM: Fast and accurate long text generation with few-step diffusion language models. In *The Fourteenth International Conference on Learning Representations*, 2026. URL <https://openreview.net/forum?id=ue1zFeD275>.
- Niels Mündler, Jasper Dekoninck, and Martin Vechev. Constrained decoding of diffusion LLMs with context-free grammars. In *The Fourteenth International Conference on Learning Representations*, 2026. URL <https://openreview.net/forum?id=7Sph4KyeYO>.
- Shen Nie, Fengqi Zhu, Zebin You, Xiaolu Zhang, Jingyang Ou, Jun Hu, Jun Zhou, Yankai Lin, Ji-Rong Wen, and Chongxuan Li. Large language diffusion models. In *The Thirty-ninth Annual Conference on Neural Information Processing Systems*, 2026. URL <https://openreview.net/forum?id=KnqjCOznVF>.
- Long Ouyang, Jeffrey Wu, Xu Jiang, Diogo Almeida, Carroll Wainwright, Pamela Mishkin, Chong Zhang, Sandhini Agarwal, Katarina Slama, Alex Ray, John Schulman, Jacob Hilton, Fraser Kelton, Luke Miller, Maddie Simens, Amanda Askell, Peter Welinder, Paul F Christiano, Jan Leike, and Ryan Lowe. Training language models to follow instructions with human feedback. In S. Koyejo, S. Mohamed, A. Agarwal, D. Belgrave, K. Cho, and A. Oh, editors, *Advances in Neural Information Processing Systems*, volume 35, pages 27730–27744. Curran Associates, Inc., 2022. URL https://proceedings.neurips.cc/paper_files/paper/2022/file/b1efde53be364a73914f58805a001731-Paper-Conference.pdf.
- Kevin Rojas, Jiahe Lin, Kashif Rasul, Anderson Schneider, Yuriy Nevmyvaka, Molei Tao, and Wei Deng. Improving reasoning for diffusion language models via group diffusion policy optimization, 2026. URL <https://arxiv.org/abs/2510.08554>.

- Subham Sekhar Sahoo, Marianne Arriola, Yair Schiff, Aaron Gokaslan, Edgar Marroquin, Justin T Chiu, Alexander Rush, and Volodymyr Kuleshov. Simple and effective masked diffusion language models. In A. Globerson, L. Mackey, D. Belgrave, A. Fan, U. Paquet, J. Tomczak, and C. Zhang, editors, *Advances in Neural Information Processing Systems*, volume 37, pages 130136–130184. Curran Associates, Inc., 2024. doi: 10.52202/079017-4135. URL https://proceedings.neurips.cc/paper_files/paper/2024/file/eb0b13cc515724ab8015bc978fdde0ad-Paper-Conference.pdf.
- Zhihong Shao, Peiyi Wang, Qihao Zhu, Runxin Xu, Junxiao Song, Xiao Bi, Haowei Zhang, Mingchuan Zhang, Y. K. Li, Y. Wu, and Daya Guo. Deepseekmath: Pushing the limits of mathematical reasoning in open language models, 2024. URL <https://arxiv.org/abs/2402.03300>.
- Richard S Sutton and Andrew G Barto. *Reinforcement Learning: An Introduction*. MIT press, 2018.
- Xiaohang Tang, Rares Dolga, Sangwoong Yoon, and Ilija Bogunovic. wd1: Weighted policy optimization for reasoning in diffusion language models. *ICLR*, 2026. URL <https://openreview.net/forum?id=L2rfd2Czjb>.
- Jonathan Uesato, Nate Kushman, Ramana Kumar, Francis Song, Noah Siegel, Lisa Wang, Antonia Creswell, Geoffrey Irving, and Irina Higgins. Solving math word problems with process- and outcome-based feedback, 2022. URL <https://arxiv.org/abs/2211.14275>.
- Zhihui Xie, Jiacheng Ye, Lin Zheng, Jiahui Gao, Jingwei Dong, Zirui Wu, Xueliang Zhao, Shansan Gong, Xin Jiang, Zhenguo Li, and Lingpeng Kong. Dream-coder 7b: An open diffusion language model for code, 2025. URL <https://arxiv.org/abs/2509.01142>.
- Zhangchen Xu, Yang Liu, Yueqin Yin, Mingyuan Zhou, and Radha Poovendran. Kodcode: A diverse, challenging, and verifiable synthetic dataset for coding, 2025. URL <https://arxiv.org/abs/2503.02951>.
- Jiacheng Ye, Zhihui Xie, Lin Zheng, Jiahui Gao, Zirui Wu, Xin Jiang, Zhenguo Li, and Lingpeng Kong. Dream 7b: Diffusion large language models, 2025. URL <https://arxiv.org/abs/2508.15487>.
- Qiyang Yu, Zheng Zhang, Ruofei Zhu, Yufeng Yuan, Xiaochen Zuo, Yu Yue, Weinan Dai, Tiantian Fan, Gaohong Liu, Lingjun Liu, Xin Liu, Haibin Lin, Zhiqi Lin, Bole Ma, Guangming Sheng, Yuxuan Tong, Chi Zhang, Mofan Zhang, Wang Zhang, Hang Zhu, Jinhua Zhu, Jiase Chen, Jiangjie Chen, Chengyi Wang, Hongli Yu, Yuxuan Song, Xiangpeng Wei, Hao Zhou, Jingjing Liu, Wei-Ying Ma, Ya-Qin Zhang, Lin Yan, Mu Qiao, Yonghui Wu, and Mingxuan Wang. Dapo: An open-source llm reinforcement learning system at scale, 2025. URL <https://arxiv.org/abs/2503.14476>.
- Siyan Zhao, Devaansh Gupta, Qinqing Zheng, and Aditya Grover. d1: Scaling reasoning in diffusion large language models via reinforcement learning. *ICLR*, 2025. URL <https://openreview.net/forum?id=t8oYNHAvM9>.
- Xinyu Zhu, Mengzhou Xia, Zhepei Wei, Wei-Lin Chen, Danqi Chen, and Yu Meng. The surprising effectiveness of negative reinforcement in llm reasoning. *arXiv preprint arXiv:2506.01347*, 2025.

Appendix

Appendix Contents

| | | |
|----------|---|-----------|
| A | Experimental details and reproducibility | 14 |
| A.1 | Hyperparameters | 14 |
| A.2 | Benchmark details | 14 |
| B | Additional method details | 16 |
| B.1 | DPS: last-step handling | 16 |
| B.2 | DPS: recording stride | 17 |
| B.3 | SML: retaining the fully-masked estimate in ratio-based methods | 17 |
| B.4 | SML: complementarity with prior variance reduction | 17 |
| C | Ablation studies and sensitivity analysis | 18 |
| C.1 | DPS record stride and last-step mode | 18 |
| C.2 | DPS normalization mode | 18 |
| C.3 | DPS modulation strength | 20 |
| C.4 | SML sensitivity: number of strata and stratification strategy | 20 |
| C.5 | SML regularization weight | 21 |
| C.6 | Computational overhead | 22 |
| C.7 | Constrained decoding: JSON generation | 22 |
| C.8 | Training Dynamics: DPS Accelerates Reward Growth | 23 |

A Experimental details and reproducibility

A.1 Hyperparameters

table 3 summarizes the training hyperparameters shared across all experiments. These settings are held constant across all three base methods (Diffu-GRPO, wd1, GDPO) and our extensions, ensuring that any performance differences are attributable to the method rather than training configuration. table 4 lists the hyperparameters specific to DPS and SML.

A.2 Benchmark details

table 5 summarizes the benchmarks, training configuration, and which DACA-GRPO components are applied. “Steps” refers to the number of optimizer updates (each step processes one batch across all GPUs with gradient accumulation). For mathematical reasoning and constraint satisfaction tasks, we follow the dataset splits and training protocols of Tang et al. (2026). For code generation tasks, we follow Rojas et al. (2026); HumanEval and MBPP is evaluation-only and we train on KodCode (Xu et al., 2025). For JSON generation, we construct a synthetic dataset from JSONSchemaBench (Geng et al., 2025).

Reward functions. Following Tang et al. (2026), we use multi-component reward functions for mathematical reasoning tasks. For MATH-500, the reward combines a format component (+1.0 for answer wrapped in `\boxed{}` with reasoning, scaled down for partial formatting) and a correctness component (+2.0 if the boxed answer matches the ground truth), yielding scores in $[0.25, 3.0]$. For GSM8K, the reward combines XML structure compliance (+0.125 per correct tag), soft and strict format matching (+0.5 each), integer answer validation (+0.5), and correctness (+2.0 for exact match), yielding scores in $[0, 3.625]$. For constraint satisfaction tasks, Countdown uses a three-level reward: +1.0 if the arithmetic expression reaches the target using exactly the given numbers, +0.1 if the correct numbers are used but the target is missed, and 0 otherwise. Sudoku uses the fraction of correctly filled empty cells as the reward, focusing on solving accuracy rather than copying given values. For code generation tasks (MBPP and HumanEval), the reward is multi-component: A binary formatting reward is used (+1.0 if output is wrapped in “python markdown fences), and a continuous reward which is the fraction of passed unit tests.

JSON generation. LLaDA-8B-Instruct, without any RL post-training, already achieves 88–96% schema adherence on existing JSON generation benchmarks such as json-mode-eval and json-mode-eval-extended Mündler et al. (2026). After applying RL, the model achieves nearly 100%, making these benchmarks unsuitable for evaluating RL for JSON generation. The primary reason for this is that these benchmarks do not have particularly complex schemas (e.g. lacking nested structures). We therefore construct a synthetic dataset from JSONSchemaBench (Geng et al., 2025), which provides a curated collection of JSON schemas organized by difficulty (github-easy, github-medium for example). For each schema, we use GPT-5 to generate three distinct scenarios that fit the schema, then for each scenario we prompt GPT-5 again with the scenario and schema to produce the corresponding JSON output. We filter out examples where the generated ground-truth JSON fails to parse or does not conform to the schema, retaining only verified (schema, scenario, JSON) triples. We preserve the original JSONSchemaBench difficulty splits and evaluate on the github-medium difficulty test split¹.

The JSON generation reward combines three components, inspired by SO-Bench (Feng et al., 2026): (1) a *format reward* (+1.0 if the output uses “json markdown fences, +0.5 if the output is valid JSON without fences, 0 otherwise); (2) a *strict schema reward* (binary +1.0 if the fenced JSON is schema-compliant, 0 otherwise); and (3) a *character-level content reward* using hierarchical field-matching accuracy based on normalized Levenshtein distance. The content reward computes field-matching accuracy between the predicted and ground-truth JSON after recursive normalization (sorting dict keys, aligning list elements), squares the score for sharper gradients, and applies a $0.8\times$ penalty multiplier when the prediction violates the schema.

¹We intend to publish this dataset to the public at a later date

Table 3 Training hyperparameters. Settings shared across all base methods (Diffu-GRPO, wd1, GDPO) and our extensions.

| Category | Hyperparameter | Value |
|------------------------|-------------------------------|----------------------|
| <i>Model</i> | | |
| | Base model | LLaDA-8B-Instruct |
| | Precision | bfloat16 |
| | Attention implementation | FlashAttention-2 |
| | Quantization | 4-bit (QLoRA) |
| <i>LoRA</i> | | |
| | Rank (r) | 128 |
| | Alpha (α) | 64 |
| | Dropout | 0.05 |
| | Task type | CAUSAL_LM |
| <i>Generation</i> | | |
| | Group size (G) | 6 |
| | Max completion length | 256 tokens |
| | Max prompt length | 200 tokens |
| | Block length | 32 |
| | Diffusion steps | 128 |
| | Remasking strategy | Low confidence |
| | Random masking | True |
| | Generation batch size | 6 |
| <i>Optimization</i> | | |
| | Optimizer | AdamW |
| | Learning rate | 3e-6 |
| | LR scheduler | Constant with warmup |
| | Warmup ratio | 0.0001 |
| | Adam β_1 / β_2 | 0.9 / 0.99 |
| | Weight decay | 0.1 |
| | Max gradient norm | 0.2 |
| | Per-device batch size | 6 |
| | Gradient accumulation steps | 2 |
| | Number of GPUs | 8 |
| | Inner iterations | 12 |
| | Gradient checkpointing | Off |
| <i>GRPO-specific</i> | | |
| | PPO clip range (ϵ) | 0.5 |
| | KL coefficient (β) | 0.0 |
| | Prompt masking probability | 0.15 |
| | Sync reference model | False |
| <i>Evaluation</i> | | |
| | Generation lengths | 128, 256, 512 |
| | Diffusion steps at eval | 64, 128, 256 |
| | Eval frequency | Every 100 steps |
| | Eval batch size (per device) | 6 |
| <i>Reproducibility</i> | | |
| | Random seed | 42 |

Table 4 DACA-GRPO hyperparameters. Settings specific to our proposed DPS and SML components. Default values are used in all main experiments unless otherwise noted; ranges are explored in the ablation studies of appendix C.

| Component | Hyperparameter | Default | Range explored |
|--|-----------------------------------|----------------|---|
| <i>DPS (Denoising Progress Scores)</i> | | | |
| | Modulation strength (λ) | 0.1 | {0.05, 0.1, 0.2} |
| | Record stride (s) | – | {1, 2, 4, 8, 16, 32} |
| | Normalization mode | Per-step | {Per-step, Trajectory, Group, None} |
| | Last-step mode | Extrapolate | {Raw, Neutral, Mean, Measured, Extrapolate} |
| <i>SML (Stratified Masking Likelihood)</i> | | | |
| | Number of strata (K) | 4 | {2, 3, 4, 5, 6, 7, 8} |
| | Regularization weight (η) | 0.1 | {0.05, 0.1, 0.2} |
| | Stratification strategy | Random | {Random, Confidence-based} |
| | Gradient checkpointing | Function-level | – |

Table 5 Training configuration. Steps denotes optimizer updates. Reward functions follow Tang et al. (2026) for math and constraint tasks. SML is excluded from Countdown and Sudoku due to the distributional mismatch discussed in section 6.

| Training set | Task type | Reward type | Steps | DPS | SML |
|--------------------------------------|------------------|----------------------|--------|-----|-----|
| MATH-500 | Math reasoning | Format + correctness | 6,000 | ✓ | ✓ |
| GSM8K | Math reasoning | Format + correctness | 7,500 | ✓ | ✓ |
| KodCode | Code generation | Format + unit tests | 6,000 | ✓ | ✓ |
| Countdown | Constraint sat. | Three-level | 7,500 | ✓ | ✗ |
| Sudoku | Constraint sat. | Per-cell fraction | 12,500 | ✓ | ✗ |
| JSONSchemaBench (our synthetic data) | Constrained gen. | Multi-component | 2,500 | ✓ | ✓ |

B Additional method details

This section provides extended discussion of design choices summarized briefly in the main text.

B.1 DPS: last-step handling

Tokens born at the final recorded denoising step T have no subsequent snapshot $S(T+1, \cdot)$ to compute a delta against (figure 5). We evaluate five strategies for handling this boundary case:

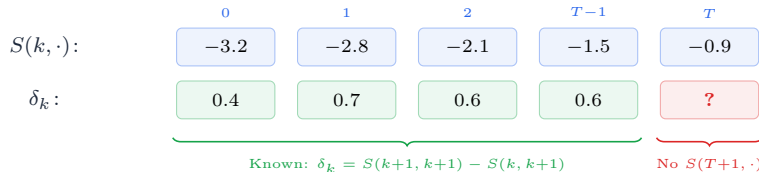


Figure 5 Last-step boundary problem. All deltas δ_k are well-defined except at the final recorded step T , where no subsequent snapshot exists to compute the difference against.

Raw Score sets $\delta_T = S(T, T)$, substituting the absolute log-probability score for the missing difference. Because all other deltas are *differences* of scores (equation (5.2)), injecting a raw score introduces a scale mismatch that distorts the per-step normalization in equation (5.3).

Neutral sets $\delta_T = 0$, effectively discarding the final step’s contribution. However, the last denoising steps are where the model resolves its most uncertain tokens; zeroing out their credit wastes precisely the signal that distinguishes difficult tokens from easy ones.

Mean sets $\delta_T = \frac{1}{T} \sum_{k < T} \delta_k$, averaging all prior deltas. This is a conservative estimator that smooths step-level noise, but it assumes roughly uniform progress across the denoising trajectory—an assumption at odds

with the non-stationary dynamics described in [equation \(5.3\)](#).

Measured computes $\delta_T = S_{\text{final}} - S(T, T)$, where S_{final} is obtained by running one additional forward pass on the fully denoised output \mathbf{x}_0 . This yields the true last-step delta but sacrifices the zero-cost property of DPS.

Extrapolate sets $\delta_T = \delta_{T-1}$, copying the second-to-last delta under the assumption that adjacent denoising transitions make comparable progress. This preserves scale consistency with other deltas (unlike Raw), retains the last step’s credit signal (unlike Neutral), requires no extra computation (unlike Measured), and makes no stationarity assumptions (unlike Mean). As shown in the ablation study ([table 6 in appendix C.1](#)), Extrapolate is the only mode that achieves the highest average accuracy at both sequence lengths while exceeding the baseline in every stride configuration (6/6). We adopt Extrapolate as the default.

B.2 DPS: recording stride

Computing DPS at every denoising step is possible but not necessarily optimal. We record snapshots every s steps (the *record stride*), capturing deltas over coarser intervals. A stride of $s=1$ provides the finest granularity but also the noisiest signal: each step un.masks only a few tokens, so the resulting delta δ_k reflects a small, potentially unrepresentative change in model belief. Larger strides aggregate more token revelations per interval, yielding higher signal-to-noise at the cost of coarser credit assignment—tokens born within the same stride window share a single delta.

The optimal trade-off is inherently task-dependent: tasks with short, structured outputs (e.g., mathematical reasoning) benefit from finer strides that distinguish individual reasoning steps, while tasks with longer, more uniform generations tolerate or even prefer coarser strides where the smoothing effect suppresses spurious fluctuations. We experimented with $s \in \{1, 2, 4, 8, 16, 32\}$ and found that the optimal stride varies across datasets; however, across nearly all configurations, the resulting attribution signal meets or exceeds the baseline—confirming that DPS is robust to this hyperparameter. A full ablation over strides and last-step modes is provided in [appendix C.1](#).

B.3 SML: retaining the fully-masked estimate in ratio-based methods

For ratio-based methods (d1, GDPO), the enriched per-token log-probability ([equation \(5.7\)](#)) averages each token’s fully-masked prediction with its stratified prediction rather than using the stratified estimate alone. Including the fully-masked term is important for two reasons.

First, it prevents a distributional mismatch between training and generation. During generation, the model starts from a fully masked state with zero inter-token context. If the importance ratio is computed entirely from stratified estimates (where each token sees $(K-1)/K$ context), the model is optimized under a regime that never occurs during actual inference. The fully-masked term anchors the ratio to the generation-time distribution.

Second, we empirically observe that using only stratified estimates degrades performance. Training becomes unstable at early stages when the model’s predictions under partial context diverge significantly from its predictions under no context. The 1/2 weighting provides a conservative blend that benefits from bias reduction while maintaining alignment with the generation regime.

B.4 SML: complementarity with prior variance reduction

Several recent methods improve estimation quality in dLLM training, but they target different sources of error at different stages of the pipeline. SML addresses *bias* in the likelihood estimate $\log p_\theta(y)$: given a completed sequence, it controls *which token positions* are masked during evaluation, ensuring each token is predicted with $(K-1)/K$ context rather than zero. DiffuCoder’s coupled sampling ([Gong et al., 2025](#)) and GDPO’s SDMC ([equation \(3.4\)](#)) instead address *variance* in the diffusion training objective: they control *which timesteps* t are used to estimate the ELBO—via antithetic pairing or deterministic quadrature, respectively. In short, SML operates on the token position axis within a single forward pass, while coupled sampling and SDMC operate on the diffusion time axis across forward passes. The mechanisms do not interfere: SML can serve

Table 6 DPS record stride and last-step mode ablation on MATH-500 with wd1 + DPS ($\lambda = 0.1$). We jointly vary the record stride $s \in \{1, 2, 4, 8, 16, 32\}$ and the last-step delta strategy. Best per-mode **bolded**. Shaded columns indicate our chosen mode.

| Stride | Raw | | Neutral | | Mean | | Measured | | Extrapolate | |
|-----------------|-------------|-------------|-------------|-------------|-------------|-------------|-------------|-------------|-------------|-------------|
| | 256 | 512 | 256 | 512 | 256 | 512 | 256 | 512 | 256 | 512 |
| 1 | 39.2 | 35.6 | 38.5 | 36.6 | 36.0 | 40.0 | 37.3 | 39.2 | 38.8 | 40.3 |
| 2 | 39.2 | 36.0 | 38.3 | 35.4 | 37.7 | 39.0 | 38.1 | 39.6 | 37.3 | 39.6 |
| 4 | 37.5 | 36.2 | 37.7 | 36.6 | 37.9 | 39.4 | 36.7 | 40.0 | 38.8 | 40.5 |
| 8 | 36.7 | 33.9 | 36.9 | 36.2 | 36.0 | 38.6 | 37.9 | 40.2 | 39.8 | 40.5 |
| 16 | 38.8 | 36.6 | 39.7 | 37.1 | 37.8 | 39.0 | 36.7 | 39.6 | 38.5 | 39.6 |
| 32 | 38.1 | 35.2 | 37.9 | 36.0 | 37.1 | 39.4 | 37.7 | 39.6 | 38.6 | 40.9 |
| wd1 baseline | 36.7 / 39.6 | | | | | | | | | |
| Avg. | 38.3 | 35.6 | 38.2 | 36.3 | 37.1 | 39.2 | 37.4 | 39.7 | 38.6 | 40.2 |
| \geq baseline | 6/6 | 0/6 | 6/6 | 0/6 | 4/6 | 1/6 | 6/6 | 6/6 | 6/6 | 6/6 |

as a drop-in replacement for the likelihood estimate inside any method that already uses coupled sampling or SDMC.

C Ablation studies and sensitivity analysis

DACA-GRPO introduces several design choices and hyperparameters across its two components. In this section we systematically evaluate each one, isolating its effect on MATH-500 with wd1 as the base method unless otherwise noted. We organize the analysis into three groups: DPS design choices covering the record stride, last-step handling, normalization mode, and modulation strength λ (appendices C.1–C.3); SML design choices covering the number of strata, stratification strategy, and regularization weight η (appendices C.4–C.5); and computational overhead, measuring the GPU memory and wall-clock cost of each component (appendix C.6).

C.1 DPS record stride and last-step mode

table 6 ablates two coupled design choices: the record stride s and the strategy for computing the final delta δ_T , where no subsequent snapshot $S(T+1, \cdot)$ exists (see equation (5.2)). We evaluate five last-step modes (see appendix B.1 for detailed descriptions):

Extrapolate is the *only* mode that achieves the highest average accuracy at both sequence lengths (38.6 at 256, 40.2 at 512) while exceeding the baseline in every stride configuration (6/6 at both lengths). Raw and Neutral both fail at length 512 (0/6 each), suggesting that scale corruption and information suppression worsen with longer sequences. Measured performs well (6/6 at both lengths) but sacrifices the zero-cost property of DPS by requiring an extra forward pass. We therefore adopt Extrapolate as the default last-step mode across all experiments.

Under Extrapolate, every stride $s \in \{1, 2, 4, 8, 16, 32\}$ exceeds the wd1 baseline at both lengths, confirming that the DPS signal is reliable across a wide range of recording granularities. The optimal stride varies slightly, but the consistent improvement over the baseline demonstrates that the attribution signal is not an artifact of a particular stride choice.

C.2 DPS normalization mode

The DPS delta δ_k (equation (5.2)) produces raw values whose scale varies systematically across the denoising trajectory: early steps operate with little context and yield small deltas, while late steps have rich context and produce larger deltas. Before these deltas enter the weight formula $\omega_i = 1 + \lambda \cdot \bar{\delta}_{\text{birth}(i)}$ (equation (5.4)), they must be normalized to ensure fair credit assignment. The choice of normalization axis—i.e., which cells

Table 7 DPS normalization mode ablation on MATH-500 with wd1 + DPS ($\lambda = 0.1$). We jointly vary the record stride $s \in \{1, 2, 4, 8, 16, 32\}$ and the normalization mode. All experiments use the Extrapolate last-step strategy. Shaded columns indicate our chosen mode.

| Stride | Trajectory | | Group | | None | | Per-step | |
|-----------------|-------------|-------------|-------------|-------------|-------------|-------------|-------------|-------------|
| | 256 | 512 | 256 | 512 | 256 | 512 | 256 | 512 |
| 1 | 36.4 | 38.8 | 36.0 | 38.3 | 36.4 | 39.0 | 38.8 | 40.3 |
| 2 | 36.7 | 38.5 | 37.9 | 39.8 | 37.1 | 38.8 | 37.3 | 39.6 |
| 4 | 37.5 | 39.6 | 37.5 | 41.0 | 39.0 | 39.4 | 38.8 | 40.5 |
| 8 | 37.9 | 39.4 | 38.3 | 40.3 | 37.5 | 39.4 | 39.8 | 40.5 |
| 16 | 36.7 | 39.4 | 36.4 | 40.9 | 37.9 | 39.8 | 38.5 | 39.6 |
| 32 | 36.2 | 40.2 | 39.4 | 39.2 | 36.9 | 40.0 | 38.6 | 40.9 |
| wd1 baseline | | | 36.7 / 39.6 | | | | | |
| Avg. | 36.9 | 39.3 | 37.6 | 39.9 | 37.5 | 39.4 | 38.6 | 40.2 |
| \geq baseline | 3/6 | 2/6 | 4/6 | 4/6 | 4/6 | 3/6 | 6/6 | 6/6 |

in the (sample \times step) matrix share a (μ, σ) pair for z-scoring—affects what “above-average progress” means. Writing $\delta_{g,k}$ for the delta of sample g at step k , we evaluate four modes:

Per-step computes a separate mean μ_k and standard deviation σ_k at each denoising step k , aggregating across all samples in the batch:

$$\bar{\delta}_{g,k} = \frac{\delta_{g,k} - \mu_k}{\sigma_k + \epsilon}. \quad (\text{C.1})$$

This automatically handles the scale difference between early and late steps: a delta is “impressive” only relative to other samples *at that same step*. The normalization answers: “At step k , which sample made the most progress compared to other samples at this step?”

Trajectory computes a separate (μ_g, σ_g) for each sample g , aggregating across all denoising steps:

$$\bar{\delta}_{g,k} = \frac{\delta_{g,k} - \mu_g}{\sigma_g + \epsilon}. \quad (\text{C.2})$$

This performs no cross-sample comparison—it only identifies which steps were most impactful *within each individual trajectory*. A step receives high weight if it stands out relative to other steps of the same sample, regardless of whether other samples also made large progress at that point. The normalization answers: “Within this sample’s trajectory, which step was the most impactful?”

Group computes a single global (μ, σ) across all samples and all steps:

$$\bar{\delta}_{g,k} = \frac{\delta_{g,k} - \mu_{\text{all}}}{\sigma_{\text{all}} + \epsilon}. \quad (\text{C.3})$$

This is the simplest mode: a delta is above average only if it exceeds the overall mean across the entire batch and all time steps. However, because early and late steps have systematically different magnitudes, late-step deltas tend to dominate the global statistics, potentially under-weighting important early-step transitions. The normalization answers: “Was this step’s progress above or below the overall average across all samples and all times?”

None skips normalization entirely, passing raw deltas directly into the weight formula: $\bar{\delta}_{g,k} = \delta_{g,k}$. This makes the modulation sensitive to the absolute log-probability scale, which varies with model architecture, vocabulary size, and sequence length—requiring careful λ tuning for each setting.

table 7 ablates the normalization mode on MATH-500 with wd1 + DPS ($\lambda = 0.1$), jointly varying the record stride $s \in \{1, 2, 4, 8, 16, 32\}$. We evaluate at generation lengths 256 and 512.

Per-step is the only mode that exceeds the baseline in all 12 stride-length configurations (6/6 at both lengths) and achieves the highest average accuracy (38.6 / 40.2). The other three modes each fail for a structural reason. Trajectory normalizes within each sample independently, forcing every trajectory to have the same

Table 8 DPS modulation strength ablation on MATH-500 with wd1 + DPS. Best accuracy (%) across record strides $s \in \{1, 2, 4, 8, 16, 32\}$. Shaded row indicates our default.

| λ | 128 | 256 | 512 |
|--------------|-------------|-------------|-------------|
| 0 (baseline) | 32.6 | 36.7 | 39.6 |
| 0.05 | 33.4 | 39.2 | 40.9 |
| 0.1 | 33.5 | 39.8 | 40.9 |
| 0.2 | 35.0 | 39.0 | 40.2 |

dynamic range regardless of whether it made meaningful progress; this washes out the cross-sample signal DPS relies on, and its average at length 512 (39.3) actually falls below the baseline. Group uses a single global (μ, σ) , which is dominated by large late-step deltas and suppresses the small but decisive early-step transitions where the model commits to key structural choices. None leaves ω_i sensitive to the absolute log-probability scale, which drifts with vocabulary size, sequence length, and training stage—making a fixed λ unstable across configurations. Per-step avoids all three failures: by computing (μ_k, σ_k) at each step independently, it adapts to the non-stationary delta scale while preserving cross-sample comparisons, and yields modulation factors bounded predictably regardless of training stage. **We therefore adopt per-step as the default.**

C.3 DPS modulation strength

The modulation strength λ in [equation \(5.4\)](#) controls how aggressively DPS reweights per-token advantages: $\lambda = 0$ recovers the base method (uniform weighting), while larger values amplify the distinction between decisive and routine denoising steps. Too small a value underutilizes the DPS signal; too large a value risks destabilizing training by assigning extreme weights to outlier deltas. [table 8](#) ablates $\lambda \in \{0.05, 0.1, 0.2\}$ on MATH-500 with wd1 + DPS, reporting the best accuracy across all record strides $s \in \{1, 2, 4, 8, 16, 32\}$ (using per-step normalization and Extrapolate last-step mode, as established in [appendices C.1](#) and [C.2](#)).

All three λ values improve over the baseline at every generation length, confirming that DPS is beneficial across a range of modulation strengths. An interesting pattern emerges across lengths: $\lambda=0.2$ is strongest at $L=128$ (+2.4pp over baseline) where aggressive reweighting helps the model focus on the few decisive steps in short outputs, while $\lambda=0.1$ is best at $L=256$ and tied-best at $L=512$ where moderate modulation avoids over-weighting noisy deltas in longer trajectories. We select $\lambda=0.1$ as the default since it achieves the best or tied-best accuracy at the two longer generation lengths, which are the more common evaluation settings, while remaining competitive at $L=128$.

C.4 SML sensitivity: number of strata and stratification strategy

[figure 6](#) ablates the number of strata $K \in \{2, \dots, 8\}$ and the stratification strategy (random vs. confidence-based) on MATH-500 across all d1 and wd1.

SML improves wd1 and Diffu-GRPO robustly. On both methods, the average accuracy across all seven K values exceeds the respective baseline at nearly every generation length. A practitioner choosing K blindly can still expect to see improvements, making SML a low-risk addition. That the pattern holds for both a ratio-free method (wd1) and a ratio-based method (Diffu-GRPO) confirms that the benefit originates from better likelihood estimation rather than from interaction with a specific loss structure.

Random stratification dominates confidence-based. Confidence-based stratification occasionally produces the single highest accuracy at a given K (e.g., $K=6$ on wd1 at $L=128$; $K=7$ on d1 at $L=128$), but its variance across K is substantially higher. This erratic behavior has a principled explanation: confidence-based sorting relies on prediction entropy from a fully-masked forward pass—the same biased regime that SML exists to correct. When entropy estimates are noisy, the resulting strata can be adversarial: hard-to-predict tokens cluster together within a stratum, depriving each other of the contextual benefit that SML is supposed to provide. Random stratification avoids this by ensuring each stratum is a representative sample of the full difficulty spectrum, yielding a smoother profile that requires less per-task tuning.

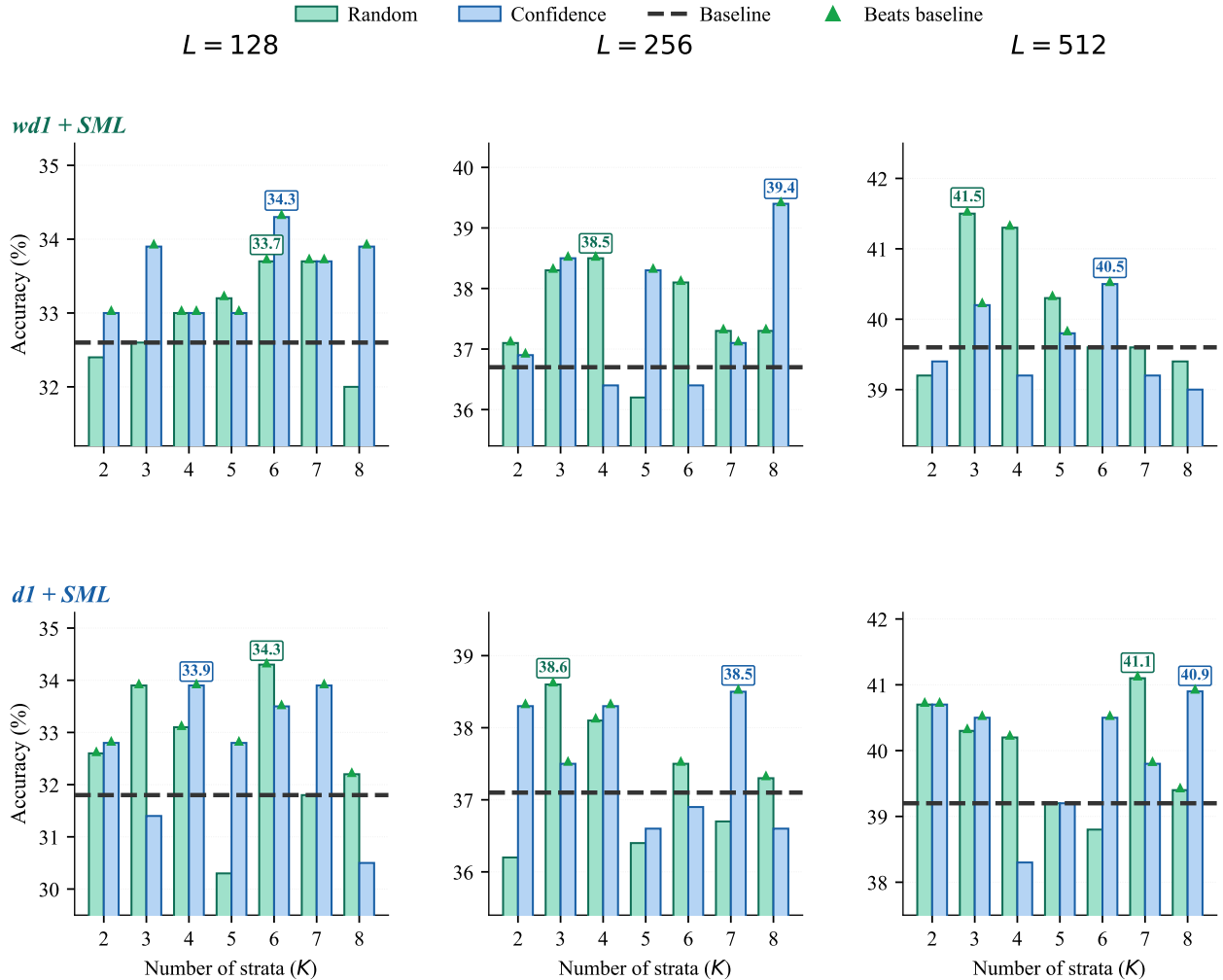


Figure 6 SML sensitivity on MATH-500 for Diffu-GRPO and wd1. Grouped bars show accuracy (%) with random (teal) and confidence-based (blue) stratification for $K \in \{2, \dots, 8\}$ at three generation lengths. Dashed lines: respective baselines without SML. Green triangles (▲) mark configurations that meet or exceed the baseline. SML consistently improves wd1 and Diffu-GRPO across most K values, with random stratification showing a smoother profile.

C.5 SML regularization weight

For ratio-free methods like wd1, SML enters the training loss as an additive regularizer weighted by η (equation (5.6)). This coefficient balances two objectives: the advantage-weighted base loss (which handles credit assignment between correct and incorrect samples) and the SML likelihood term (which improves token-prediction quality under richer context). Too small an η renders SML ineffective; too large an η lets the SML term dominate the base loss, reducing the influence of the reward signal.

table 9 ablates $\eta \in \{0.05, 0.1, 0.2\}$ on MATH-500 with wd1 + SML, reporting the best accuracy across all strata counts $K \in \{2, \dots, 8\}$ and both stratification strategies. All three η values improve substantially over the baseline at every generation length (+1.4–1.9pp average gain), confirming that SML is beneficial across a wide range of regularization strengths. The spread between worst and best η at any given length is small: 0.3pp at $L=128$, 0.8pp at $L=256$, and 0.4pp at $L=512$. This insensitivity is a practical advantage—a practitioner can adopt $\eta=0.1$ without per-task tuning. We select $\eta=0.1$ as the default since it achieves the best or tied-best accuracy at all three generation lengths.

Table 9 SML regularization weight ablation on MATH-500 with wd1 + SML. Best accuracy (%) across $K \in \{2, \dots, 8\}$ and both stratification strategies. Best per-length **bolded**. Shaded row indicates our default.

| η | 128 | 256 | 512 |
|--------------|-------------|-------------|-------------|
| 0 (baseline) | 32.6 | 36.7 | 39.6 |
| 0.05 | 34.0 | 39.0 | 41.4 |
| 0.1 | 34.3 | 39.4 | 41.5 |
| 0.2 | 34.3 | 38.6 | 41.1 |

C.6 Computational overhead

All experiments are conducted on a cluster of $8 \times$ NVIDIA H100 80GB GPUs using QLoRA (4-bit quantization with LoRA rank 128). We measure the overhead of DPS and SML independently on top of the wd1 base method, running 100 training steps with the default configuration (table 3).

Table 10 Computational overhead of DPS and SML. Wall-clock time measured over 100 training steps on wd1 with LLaDA-8B-Instruct. Overhead (%) is relative to the wd1 baseline.

| Configuration | Wall-clock (s) | Overhead (%) |
|--|----------------|--------------|
| <i>Baseline</i> | | |
| wd1 | 3 768 | — |
| <i>DPS (varying record stride s)</i> | | |
| $s = 1$ | 3 887 | +3.2 |
| $s = 4$ | 3 797 | +0.8 |
| $s = 16$ | 3 785 | +0.5 |
| $s = 32$ | 3 771 | +0.1 |
| <i>SML (varying number of strata K)</i> | | |
| $K = 2$ | 4 014 | +6.5 |
| $K = 4$ | 4 208 | +11.7 |
| $K = 8$ | 4 590 | +21.8 |

table 10 presents the wall-clock time across varying DPS record strides and SML strata counts and reveals two patterns.

DPS is near-zero cost. Wall-clock overhead scales linearly with the number of recorded snapshots (T_{diff}/s): from +0.1% at $s=32$ (4 snapshots per trajectory) to +3.2% at $s=1$ (128 snapshots). At our recommended operating range of $s \in \{4, 8, 16, 32\}$, the overhead is under 1%—negligible relative to the $G \times T_{\text{diff}} = 6 \times 128 = 768$ generation-phase forward passes that dominate each training step.

SML scales linearly with K . Wall-clock overhead is +6.5% at $K=2$, +11.7% at $K=4$ (our default), and +21.8% at $K=8$, consistent with K additional forward passes per inner iteration during loss computation. Even at $K=4$, the overhead is modest: loss computation accounts for a small fraction of each training step compared to the generation phase. Since DPS and SML operate in different phases of the training loop—DPS during generation, SML during loss computation—their overheads are additive and non-interacting.

C.7 Constrained decoding: JSON generation

table 11 reports Schema Adherence Rate on the GITHUB-MEDIUM JSON benchmark, which is the fraction of outputs that conform to the target schema. Note that the output conforming to the schema implies that it also parses as valid JSON. We evaluate Diffu-GRPO and wd1 at $L=512$ and GDPO at $L=256$ (since the implementation of GDPO for the JSON task runs into OOM issues with $L=512$). For each method we report the best accuracy across all record strides $s \in \{1, 2, 4, 8, 16, 32\}$ (for DPS) or strata counts and stratification strategies (for SML).

Analysis. Two patterns are notable. First, DACA-GRPO achieves the highest improvement on wd1 (+5.90pp) and GDPO (+3.82pp), with both DPS and SML contributing complementary gains—on wd1, DPS alone adds +3.47pp and SML alone adds +3.82pp, while the combination exceeds both at +5.90pp.

Table 11 JSON generation results. Schema Adherence Rate (%) on GITHUB-MEDIUM. Diffu-GRPO and wd1 evaluated at $L=512$; GDPO at $L=256$. Best accuracy across record strides (for DPS) or strata counts and stratification strategies (for SML) reported. Green values show absolute change over the reproduced baseline. Blue rows are our methods.

| Method | Schema Adherence (%) | |
|-------------------------------|----------------------|-------|
| LLaDA-8B-Instruct ($L=256$) | 48.83 | |
| LLaDA-8B-Instruct ($L=512$) | 60.55 | |
| Diffu-GRPO ($L=512$) | 69.44 | |
| + DPS | 73.96 | +4.52 |
| + SML | 71.18 | +1.74 |
| + DACA-GRPO | 73.61 | +4.17 |
| wd1 ($L=512$) | 72.57 | |
| + DPS | 76.04 | +3.47 |
| + SML | 76.39 | +3.82 |
| + DACA-GRPO | 78.47 | +5.90 |
| GDPO ($L=256$) | 63.19 | |
| + DPS | 64.23 | +1.04 |
| + SML | 65.28 | +2.09 |
| + DACA-GRPO | 67.01 | +3.82 |

On d1, DPS alone (+4.52pp) slightly outperforms DACA-GRPO (+4.17pp), suggesting mild interference between the two components under the ratio-based formulation for this task.

Second, unlike the short-output constraint satisfaction tasks (Countdown, Sudoku) where SML caused mode collapse (Section 6), SML is effective on JSON generation despite JSON being a structurally constrained format. This confirms that SML’s failure on constraint tasks is driven by *output length*, not by the presence of structural constraints: JSON outputs at $L=512$ are long enough that revealing 75% of the sequence does not trivially determine the remaining tokens, so the SML gradient teaches useful predictive skills that transfer to generation. This result sharpens the applicability boundary of SML: it is effective whenever the output is sufficiently long and semantically diverse, regardless of whether the task imposes structural constraints.

C.8 Training Dynamics: DPS Accelerates Reward Growth

To understand *when* during training DPS contributes, we compare reward trajectories of wd1 and wd1 + DPS on three representative benchmarks: Countdown, MATH-500, and Sudoku (figure 7). Reward is the per-step group mean, smoothed with a 20-step rolling window; shaded bands denote \pm one group standard deviation. Each pair shares the same seed, batch size, generation length, and reward functions, so the only difference is whether the per-token advantage is modulated by $\bar{\delta}_{\text{birth}(i)}$.

DPS On Countdown and Sudoku, the wd1 + DPS curves separate from the baseline within the first few hundred steps and continue widening throughout training, ending at +0.302 (+84.7%) and +0.356 (+74.0%) absolute mean reward respectively. Both tasks have tight inter-token dependencies (arithmetic operators, grid constraints) so *which* denoising step commits the model to a particular structural choice matters disproportionately—the precise signal that uniform credit assignment dilutes and that DPS recovers.

On MATH-500 the gap is smaller but consistent. The two curves co-evolve early on—both methods learn the same easy reward shaping—but wd1 + DPS pulls ahead in the second half of training and ends +0.058 (+4.2%) above baseline. Long, free-form math completions contain more routine fill-in tokens (whitespace, repeated digits, formatting), so the fraction of steps with high δ_k is lower; the residual gain comes exclusively from the small subset of decisive steps that DPS up-weights. This is consistent with our results in table 1, where SML—targeting the orthogonal weakness of biased likelihood estimates—provides the complementary gains on long-form math reasoning.

Stability. Across all three datasets, wd1 + DPS exhibits no additional variance: the shaded bands track the

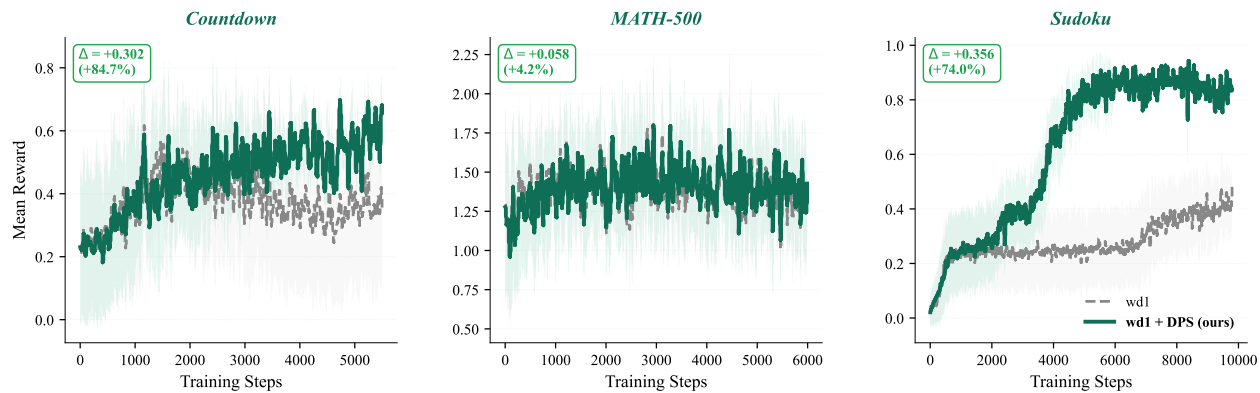


Figure 7 Training dynamics: wd1 vs wd1+DPS. Mean reward (solid lines) with ± 1 group std (shaded bands), smoothed over a 20-step rolling window. DPS produces an immediate and persistent gap on the structured benchmarks (Countdown, Sudoku) and a smaller but consistent gain on MATH-500. The Δ box reports the absolute and relative final-reward improvement. All runs use identical hyperparameters except for the DPS modulation.

baseline closely and the mean curve is monotone after smoothing. This supports our claim that DPS is a *plug-and-play* modification—it modulates the existing advantage rather than introducing new gradient sources, so it cannot destabilise the trust region or amplify reward variance.